8-2016

A Real-Time Programmable Pulsatile Flow Pump for In-Vitro Cardiovascular Experimentation

Rahul Raj Mechoor
Clemson University

A REAL–TIME PROGRAMMABLE PULSATILE FLOW PUMP FOR IN-VITRO CARDIOVASCULAR EXPERIMENTATION

A Thesis
Presented to
the Graduate School of
Clemson University

In Partial Fulfillment
of the Requirements for the Degree
Master of Science
Mechanical Engineering

---

by
Rahul Raj mechoor
August 2016

Accepted by:
Ethan Kung, PhD, Committee Chair
Richard Figliola, PhD
Georges Fadel, PhD

ABSTRACT

Benchtop In-vitro experiments are valuable tools for investigating the cardiovascular system and testing medical devices. Accurate reproduction of physiologic flow waveforms at various anatomic locations is an important component of these experimental methods. This study discusses the design, construction and testing of a low-cost and fully programmable pulsatile flow pump capable of continuously producing unlimited cycles of physiologic waveforms. Two prototypes with different designs were tested. The first one consisted of a stepper motor – piston pump combination and tests showed that it failed to satisfy the design requirements. The second, highly successful prototype consists of a gear pump actuated by an AC servo-motor and a feedback algorithm enabling high accuracy for flow rates up to 300ml/s across a range of loading conditions. The iterative feedback algorithm uses flow error values in one iteration to modify motor control waveform for the next iteration to better match desired flow. Within 4-7 iterations of feedback, the pump replicated physiologic flow waveforms to high levels of accuracy (normalized RMS error less than 2%) under varying downstream impedances. This device is significantly more affordable (~10% of the cost) than current commercial options. Furthermore, the pump can be controlled via common scientific software packages and thus can be implemented in large automation frameworks.

ACKNOWLEDGMENTS

I would like to thank everybody who helped me get through this thesis and the two years of my Masters in Clemson University.

Especially, I would like to thank Dr. Ethan Kung for providing me with valuable guidance, inspiration and motivation. He has been an excellent mentor personally and in academia.

I would like to thank my committee members Dr. Richard Figliola and Dr. Georges Fadel for all the guidance and cooperation.

This project would not have been possible without the assistance of all the staff of the mechanical engineering department, Michael Justice, Jamie Cole, Stephen Bass, Gwen Dockins, Corbin Kolehmainen, Katherine Poole and Trish Nigro.

I am deeply thankful to my lab mates Tyler Schmidt, Fei He, Akash Gupta, Masoud Farhamand and Ehsan Misraei for their assistance and companionship.

Last but not least, I would like to thank my parents, grandparents and friends for providing me the strength to continue my journey.

TABLE OF CONTENTS

Page

Table of Contents (Continued)

Page

LIST OF FIGURES

List of Figures (Continued)

Figure Page

CHAPTER ONE

INTRODUCTION

Motivation

Cardiovascular diseases are the leading causes of death around the world. According to the American Heart Association, more than 7.6 million cardiovascular procedures were performed in the US with the total treatment spending exceeding $320 billion in 2011 [1]. From these facts, it is evident that cardiovascular science is a field that has a lot of potential and need for growth. It has been shown that quantities such as three dimensional blood flow velocities and stress and strain in blood vessels are the most important parameters in the initiation and progression of cardiovascular diseases like aneurysms [2]. The difficulty of clinically measuring these important quantities is one of the biggest roadblocks in cardiovascular studies. Ethical considerations also present challenges to progress since extensive data collection directly from patients is undesirable. As a solution to these problems, engineering approaches such as benchtop in-vitro experiments or computational simulations have been used where physiological conditions can be recreated for detailed investigation. While computational methods can offer detailed quantifications of hemodynamic parameters, transient cases can be very resource intensive and modeling of complex fluid-structure interactions such as device implementation remains challenging. Experimental methods offer the ability to recreate physical interactions that are currently difficult for computational methods and serve as useful platforms for biomechanics investigation and medical device testing.

Bench top cardiovascular experimentation is an area that could bring about tremendous changes in current procedures, treatment and medical device testing. It entails the use of medical imaging techniques and the knowledge of fluid mechanics to recreate physiologically realistic anatomy, pressure, and flow on a bench top circuit. This enables extensive in vitro testing of medical devices, aids the study of the nature and impact of different vascular defects and surgical procedures, and helps in creating a better overall understanding of the dynamics of our vascular system. The most impressive feat of cardiovascular experimentation is that we achieve all this without any risk and minimal discomfort to patients.

Current State of the Art: Literature Study

The most important component of a bench top test setup is a pulsatile pump, capable of producing physiologically realistic flow and pressure since it is impossible to analyze the fluid mechanics of the circulatory system without replicating the pulsatile nature of blood flow. A flow source, usually a positive displacement pump, creates a pulsatile flow waveform which then feeds into downstream impedances. The downstream impedances typically consist of circuit elements, such as flow resistors and compliance chambers, to mimic vascular impedance and result in realistic pressure waveforms.

One approach to recreating physiologic conditions uses one or multiple pumps to recreate cardiac flow, and a downstream vascular simulator, which recreates the impedances along the whole arterial tree, to obtain the desired flow waveform at specific anatomic locations. In this approach the flow source produces a pre-configured cardiac

flow waveform with varying period lengths. Commercial products, such as the 'Harvard pump' (Harvard Apparatus, Holliston. MA, USA) and the 'SuperPump' (Vivitro Labs, Victoria, BC, Canada), are designed to operate as flow sources in this approach [3,4]. When the physiological flow is reproduced in such detail for the whole body, the setup is often called a bioreactor. The main disadvantage of a bioreactor is the complexity and construction time required to build the vascular simulator. Figure 1.1 shows the electrical equivalent schematic for a bioreactor where the chambers of the heart are simulated using separate devices (shown in the red square) and the vascular simulator recreating aortic and venous flow in detail.

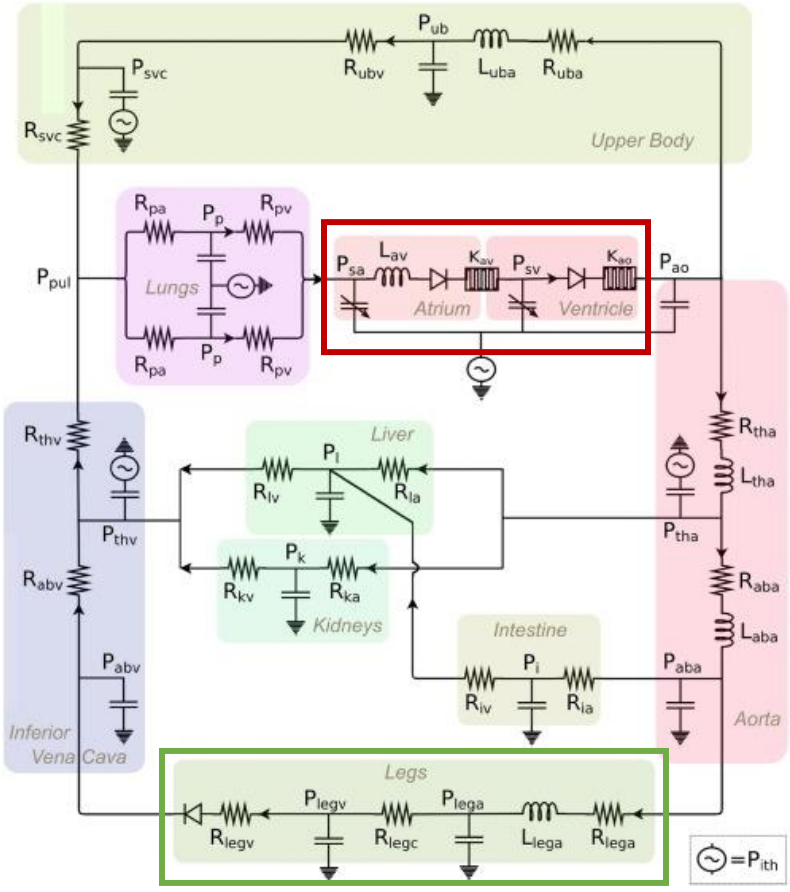

Figure 1.1: Schematic of a Bioreactor[5]

In this case if one is only interested in aortic flow in the abdominal region (shown in the green square), it is desirable to eliminate all the other circuit elements. This requires a device such as 'CardioFlow' (Shelley Medical Imaging Technologies, London, ON, Canada), that can recreate localized flow at the point of interest[6], which eliminates the need for a vascular simulator.

Figure 1.2 shows how such a device simplifies the experimental circuit compared to a bioreactor. However, there are several drawbacks to this commercial pump. First, the output flow waveform may be affected by the varying downstream loading conditions and result in imprecise waveform reproduction. Second, the pump must be controlled by a dedicated computer and stand-alone software, which inhibits direct communication with other devices or programs. Third, with the price of a single unit ranging from $15,000 to $40,000, cost is a prohibitive factor, especially in experiments that require multiple flow sources.

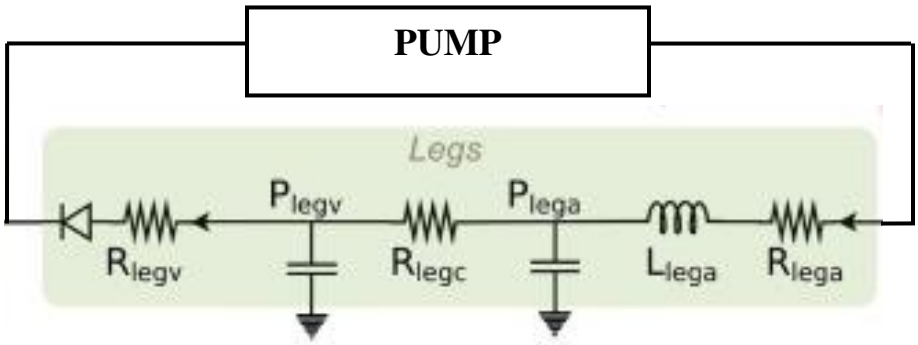

Figure 1.2: Schematic of experimental circuit using a pump producing localized flow waveforms

These facts point to a need for a custom made pulsatile pump for experimental circuits. Several previous studies have attempted to design a flow pump to reliably reproduce a wide range of localized physiological waveforms with high accuracy while maintaining low cost and complexity.

Frayne et al. [7] made one of the first notable attempts to create such a device. They designed a piston pump with a double acting cylinder capable of flow rates up to 30ml/s. This device was mainly intended for MR flow verification and calibration. This device had limited continuous operation capability and the results were largely varying according to the type and length of tubing used. Hoskins et al. [8] designed a setup with a gear pump connected to a stepper motor. But again, the flow ranges were very limited (<20ml/s).

A progressive cavity pump was used by Eriksson et al. [9] to produce uninterrupted physiologic waveforms and results were shown for the reproduction of a carotid waveform. This system is more expensive due to the use of the progressive cavity pump and it required a separate controller with its own standalone system eliminating the possibility of system integration. Tsai et al. [10] designed a more complex setup consisting of a gear pump producing constant flow, a piston pump producing the oscillating component, and a back pressure valve to avoid reverse flow into the gear pump but again testing data shown is mainly limited to a carotid waveform.

Almost all of these pumps worked under a limited operating range in terms of peak flow, few successfully demonstrated the capability of producing a physiological waveform with portions of backflow and most studies lack enough results to

convincingly exhibit the versatile performance capabilities of the pump in a physiologically realistic experimental setup. Also, there remains the need for a programmable pulsatile flow pump that can be implemented into large automation frameworks. One of the main requirements for such a pump would be the ability to communicate with computational programs written in commercial software packages and the ability to change the output flow waveform in real time with minimal human intervention.

Research Objective

The aim of this study is to design, construct and comprehensively test a simple, fully programmable pulsatile flow pump that can consistently and accurately reproduce a wide range of localized physiological flow waveforms. Evaluating experiments are designed to comprehensively test the performance of the pump in a basic level, characterizing the performance parameters such as peak flow, acceleration and accuracy and in an application level, proving the capability of the pump to recreate flow waveforms in physiologically realistic conditions. The pump is designed to be integrated with commercial software to facilitate automation. The simplicity, affordability and improved performance of this design will enable the advancement of cardiovascular medical technologies.

Organization of Thesis

This document is arranged into five chapters. The current chapter introduces the basic ideas and motivation behind the study, looks at the current state of the art in the

field and establishes the need for further investigation. The second chapter outlines the basic design ideologies, tools and processes used in the study. This section also provides a broad idea of the experimental setup and devices used. The third and fourth chapter discusses the design, construction, working principles and test results for two prototypes created as a result of this study. The fifth chapter provides an overall summary. This section also discusses the general direction for future studies. All the detailed data sheets and specifications for parts and tools used in the study are included in the appendix.

CHAPTER TWO

METHODS

Experimental setup

The basic bench top cardiovascular experimental setup consists of a closed loop flow circuit as shown in figure 2.1. It consists of a reservoir that holds the bulk of the working fluid, a pump that creates the desired flow, a test section where anatomical models can be connected and measurements are taken, and a Resistor – Capacitor – Resistor (RCR) module that creates physiologically realistic pressure downstream of the pump[11]. A 40% Glycerin solution is used as the working fluid since its physical properties like viscosity and density are similar to that of human blood. In this study, the reservoir is connected to the flow pump using flexible PVC tubing with 3/4" internal diameter. Tygon tubing with 3/8" internal diameter is used to connect the pump to the test section, RCR module, and the reservoir. This tubing was chosen since it is a requirement for the flow measurement system we used and using the same tubing reduces the need for tubing connectors that introduce additional flow disturbance and pressure drop.

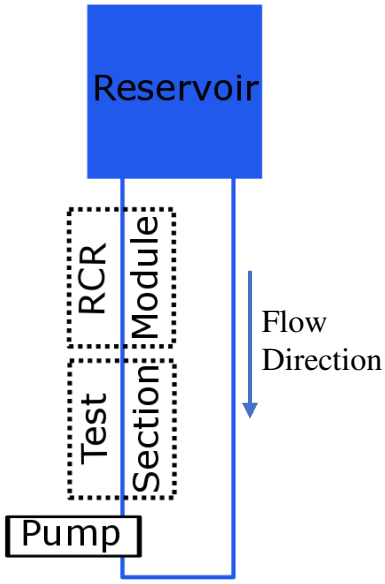

Figure 2.1: Schematic of a bench top experimental circuit

An ultrasonic transit time flow meter (TS 410 with ME-9PXL flow sensor, Transonic Systems Inc., Ithaca, NY) with a low pass filter set at 40 Hz is used to measure instantaneous flow rates at the test section. A pressure transducer (Argon DTX Plus, Argon Medical Devices Inc., Plano, TX, USA) with a pressure control unit (Millar PCU-2000, Millar, Inc., Houston, TX, USA) is used to measure pressure. Both these sensors are connected to the data acquisition system connected to the PC.

Data Acquisition and Signal Generation

Control signal generation and data acquisition is carried out using LABVIEW software package (National Instruments, Austin, TX, USA) through separate modules (NI 9205, NI 9263, National Instruments, Austin, TX, USA) on a compact DAQ chassis (NI cDAQ 9174, National Instruments, Austin, TX, USA). NI 9205 is the analog input module which receives the measured signals from flow and pressure sensors as analog

voltages. NI 9263 handles the analog voltage signal generation. NI 9401 is a digital module that can output timed counter output pulses.

The LABVIEW program acts as the interface between the user and the device. The front panel of the LABVIEW program is shown in figure 2.2. As seen there, the desired waveform can be selected from a saved file (containing flow rate values) using the 'Waveform Input File Path' dialog. The period of the waveform and number of waveforms to be produced can be selected using the corresponding options below the 'Waveform Input File Path' dialog. It also has options to average the results over a user defined number of cycles and to discard initial waveforms which might have disturbances. After the desired waveform is replicated, the program writes both raw data from the sensor and processed data into a file chosen by the user.

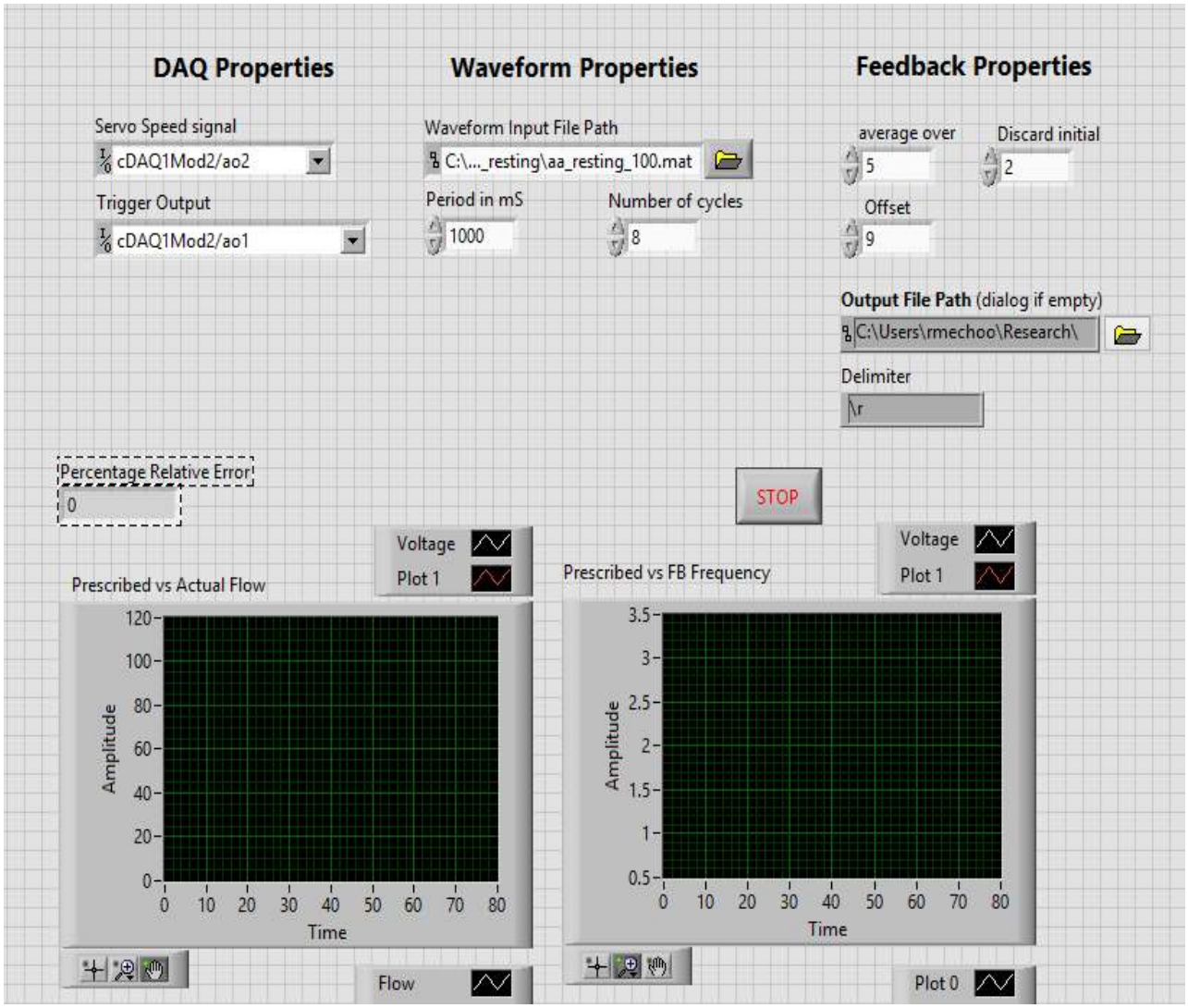

Figure 2.2: Front panel of LABVIEW program

Once the desired waveform data is fed to the program, it converts the data into output signals according to the type of pump being used. More details of this process is provided in chapter 4. This output signal controls the motor and creates an initial flow. This initial flow is always slightly different from the desired flow due to compliance in the tubing and inaccuracies in signal output and motor control. A semi – real time

feedback algorithm is used to reduce this error and better match output flow to desired flow.

Feedback Algorithm

The feedback algorithm uses a semi - real time iterative process to reduce the error in the output flow. When a desired flow waveform is prescribed, it is processed in a feedback loop until the error in the output waveform is within a user specified limit. This is achieved via a proportional error control that uses the measured error in each iteration to modify the corresponding motor control signal for the next iteration. This is shown in figure 2.3.

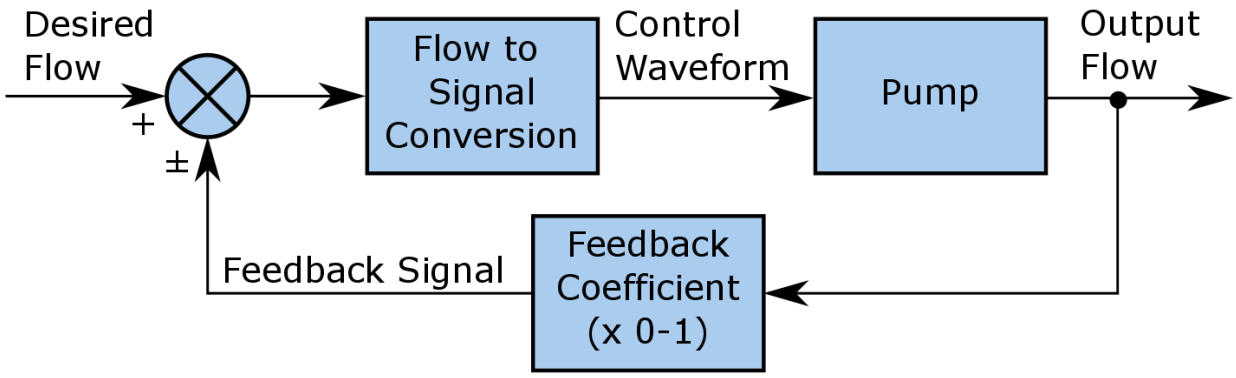

Figure 2.3: Flowchart for the feedback algorithm

Initially, when the output flow waveform is produced, the program averages the output flow over a user specified number of cycles and compares it to the desired flow waveform to find the error in flow at each data point. This error is multiplied with a feedback coefficient and fed back to the system to compensate for the error in flow. This process is repeated multiple times till the error in output flow is less than a user specified

value. The feedback coefficient is a value between 0 and 1 which specifies how fast the output flow will converge. If the value is set as 0, the feedback algorithm will have no effect. If this value is set too high, it may cause oscillations and instability in the algorithm leading to an increase in flow error. In most cases, 0.3 was found to be the best value.

General Design Ideals

The design of prototypes started from deciding the type of pump and motor to be used while the control system and other components like tubing and valves were selected based on this initial choice. The project objective, budget, level of machining required and availability of parts all played a role in the selection of each part.

While choosing the pump the most important factor was the pump's ability to reproduce flow waveforms accurately irrespective of downstream conditions. This is better accomplished by positive displacement pumps like piston pumps, gear pumps, and progressive cavity pumps, compared to rotodynamic pumps like centrifugal pumps. The next step of selection involved comparison of complexity, cost and availability. With these considerations, piston pumps and gear pumps were selected as the two final options since progressive cavity pumps are much more costly and harder to find for the required flow ranges. Comparing these two options, gear pumps were found to be easily available, simpler and more reliable whereas piston pumps were easier to build.

Stepper motors and Servo motors were the two options for the choice of actuator. Stepper motors are comparatively cheaper but servo motors are more powerful, faster and more accurate. Matching the motor performance to the speed and torque requirements of

the selected pumps, it was found that the gear pump was better suited to work with faster and more powerful servo motors while stepper motors could work with the piston pump. This created the possibility of two prototypes, the piston pump – stepper motor combination (prototype-1) which would be more affordable but possibly with lesser reliability and versatility, and the gear pump – servo motor combination (prototype-2) which would be more expensive but with the potential for higher reliability, simplicity and versatility. It was decided that prototype-1 would be built first and prototype-2 would be built only if ptrototype-1 had significant shortcomings.

Testing

A series of tests were conducted to benchmark the prototypes. An initial flow calibration was performed where the pump was operated at constant speeds with and without a downstream resistance to check the linearity of the pump output flow with respect to motor RPM and its dependence on downstream conditions. An acceleration test was conducted to ascertain the maximum possible flow acceleration. Then, a feedback test was conducted to evaluate the feedback loop by analyzing the change in output flow waveform after each feedback iteration. The abdominal aortic waveform under resting condition was used to test the capability of the pump to produce complex physiologic waveforms containing backflow. We demonstrated the pump's performance in an experiment featuring physiological flow and pressure waveforms. The cycle-to-cycle consistency in output flow was evaluated by superposing multiple waveforms without averaging and finding the maximum deviation between the cycles.

The reference physiological waveforms used are abdominal aortic flow and pressure waveforms under exercise (figure 2.4a) and resting conditions (Figure 2.4b) as reported by Kung et al. [12]. The abdominal aortic flow waveform under exercise condition is representative of a high flowrate condition, whereas the resting waveform is representative of one with back flow and high frequency, low amplitude oscillations.

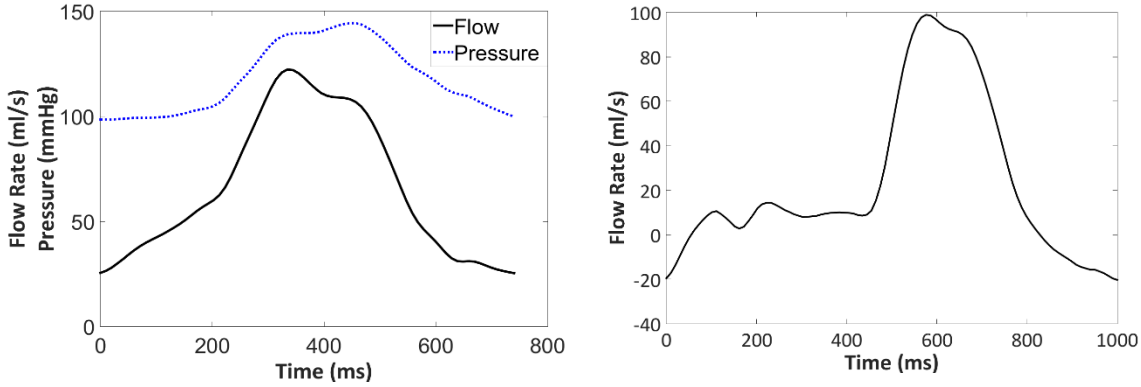

Figure 2.4a: Abdominal aortic flow and pressure under light exercise condition

Figure 2.4b: Abdominal aortic flow under resting condition

CHAPTER THREE

PROTOTYPE – 1

Design and Working Principles

Prototype-1 is shown in figure 3.1a. It consists of a piston – cylinder assembly, a stepper motor linear actuator, stepper driver and power supply. The cylinder also acts as the reservoir and is made of transparent acrylic material, with an internal diameter of 4.75 inches and length of 36 inches. The piston made of high density poly ethylene has two Viton O-rings and is bolted onto the linear nut on the actuator. The stepper motor linear actuator (E87H4, HaydonKerk motion solutions, Waterbury, CT) has a linear nut and lead screw arrangement. The lead screw is driven by the stepper motor, controlled by the driver (DCM8054, HaydonKerk motion solutions, Waterbury, CT) which receives the control signals from the NI 9401 digital output module and NI 9263 analog voltage output module. Control signals are generated by the computer using LABVIEW. The total cost of the prototype including the parts and machining is estimated to be around $1400.

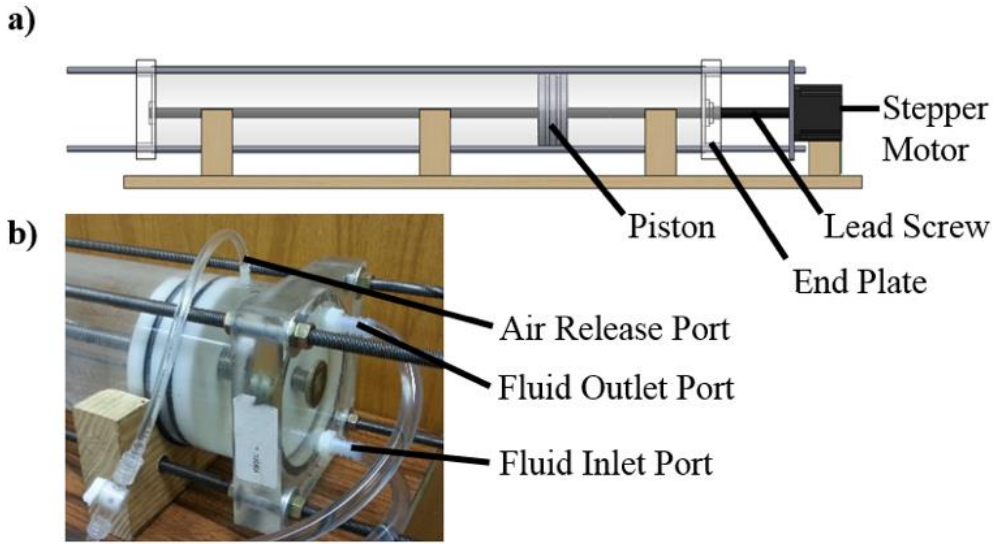

Figure 3.1a: SOLIDWORKS rendering of the pump;

Figure 3.2b: Cylinder end and connectors

The cylinder is divided into two chambers by the piston, creating a double acting pump. Cylinder ends are sealed with acrylic end plates which also houses the fluid flow ports, seals and bearings for the lead screw. Fluid ports are barbed connections on the outward facing side of end plates, almost in line with the cylinder inside wall with inlet port on top and outlet port on the bottom. As shown in figure 3.2b, air release ports are located on the top of the cylinder's curved surface, at points close to the end plates. This arrangement makes sure that any air bubbles in the system are always forced towards the air release port. Corresponding ports from both sides are connected together to form common pump inlet and outlet, controlled by three way valves.

The actuator velocity is controlled by a counter output signal from NI 9401 module. Varying the counter frequency varies the velocity of the actuator and that

changes the flow rate. The counter frequency is varied in timesteps of 10mS in most of the trial cases, providing the operator with 100 data points per second enabling the creation of any desired waveform with high accuracy. One pulse from the counter output moves the piston by 0.00125" and the velocity of the piston movement is obtained using equation 2 and consequently, the flow rate is obtained using equation 3.

$$Piston\ Velocity\left(^{in}/_{s}\right) = \ Pulse\ Train\ Velocity\ \left(^{pulses}/_{s}\right) * 0.00125 \tag{2}$$

$$\begin{aligned} Flow\ Rate\left(^{ml}/_{s}\right) \\ = \ Pulse\ Train\ Velocity\ \left(^{pulses}/_{s}\right) * 0.00125 \\ * Cross\ section\ area\ of\ cylinder \end{aligned} \tag{3}$$

The direction of piston movement is selected using an analog signal from NI 9263 module. An analog voltage of +5V selects the direction away from the motor and 0V selects the direction towards the motor. These two signals working in conjunction creates the desired flow waveforms, even ones with a back flow. One drawback of this method is the restriction on minimum frequency value imposed by the working mechanism of the output module. For the proper output of frequency waveform, every frequency value is limited so that at least one complete pulse is executed before the frequency can be changed again. This limits the minimum frequency value to the inverse of the timestep duration.

Parts Selection and Sizing

All materials used for construction of the prototype were carefully selected so that they are easy to machine and compatible with the glycerin – water solution. The acrylic cylinder allows for a clear view of the piston and O-rings which is vital for troubleshooting. For the O-rings, multiple materials like EPDM, Teflon and Viton were tested before finalizing the use of Viton due to its optimal mix of stiffness and low friction. Having two O-rings on the piston allows for better piston stability and sealing.

The piston and cylinder (4.75" internal diameter) are optimally sized to produce a peak flow rate of 200ml/s while ensuring a high flow resolution of 1.44ml/full step of the actuator. This resolution can be further enhanced by using the micro stepping feature, which allows the actuator to further reduce the step angle. The length of the cylinder (36") was chosen so that the pump is able to produce around 50 continuous cycles of the prescribed waveform before the piston reaches one end and the flow gets disturbed while the direction of motion changes and valves are adjusted accordingly.

The diameter of the piston, downstream pressure and pressure drop across tubing and connectors dictate the amount of pressure force on the face of the piston and hence the amount of thrust the actuator needs to produce. With the diameter of 4.75", downstream pressure of 200mmHg (3.87psi) and an assumed pressure loss of 200 mmHg, the total pressure force acting on the piston is calculated to be around 138lbs (equation 4). Assuming a frictional force of 50lbs (from experimental values), the total thrust required was found to be around 190lbs. The actuator should be able to produce this thrust while

producing the required velocity and acceleration to accurately reproduce the desired flow waveform. To ascertain this, velocity and acceleration profiles for the abdominal aortic waveform under exercise condition were calculated (equation 5, equation 6) and sent to the technicians at various linear actuator suppliers and the HaydonKerk E87H4(C) was found to be the best choice. It produces a thrust of more than 200lbs with a lead/step of 0.00125" at a linear velocity of 0.75inches/s. This piston velocity can produce a flow rate of 217ml/s, thus fulfilling the criteria of peak flow rate. Detailed specifications of the actuator is included in appendix.1.

$$Pressure\ force = Piston\ face\ area * Pressure\ inside\ cylinder \tag{4}$$

$$Piston\ velocity = Required\ flow\ rate / Cylinder\ cross\ section\ area \tag{5}$$

$$Piston\ acceleration = \frac{d(Piston\ velocity)}{dt} \tag{6}$$

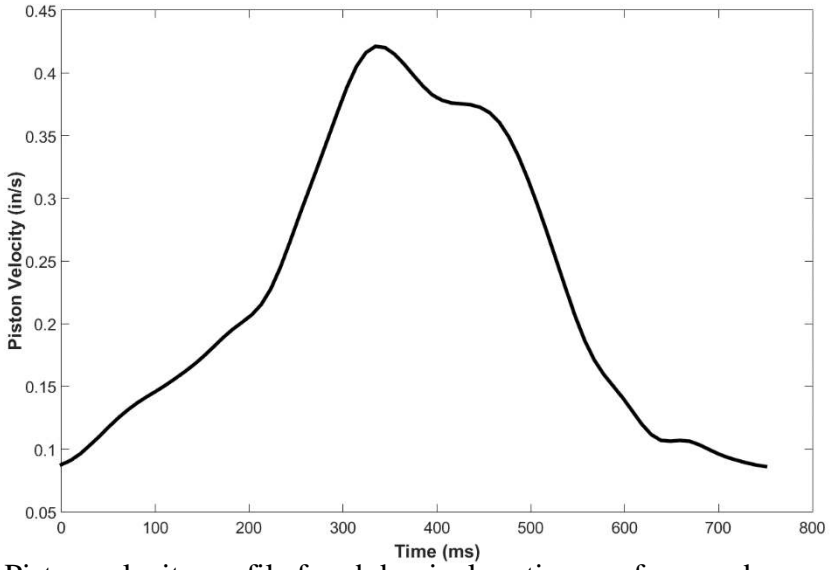

Figure 3.2: Piston velocity profile for abdominal aortic waveform under exercise condition

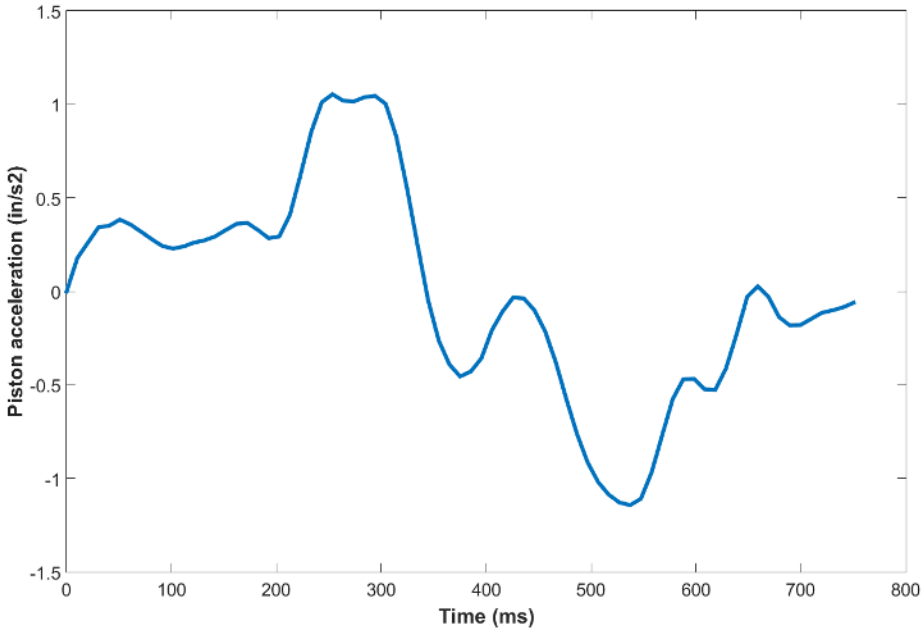

Figure 3.3: Piston acceleration profile for abdominal aortic flow waveform under exercise condition

Results

The prototype performed well during initial tests. It was able to produce the desired flow waveform with less than 2.46% mean error (figure 3.4) in flow rate at low downstream pressures. But as the prototype went through multiple hours of duty and when the downstream pressure was increased, it was unable to produce the flow peaks as required. Figure 3.5 shows an example where the actuator skipped steps and the peak of the waveform was distorted. This was mainly due to an increase in friction at the O-rings due to the slight change in shape and fit that occurred during pump operation. This increase in load combined with the pressure load overloaded the actuator and caused it to skip steps, resulting in a distorted waveform. The slight eccentricity and inaccurate

dimensions of the cylinder were contributing factors to this O-ring degradation. As a result, it was decided that this prototype is more suitable for steady flows and waveforms with lower flow rates. Since the prototype failed to produce the required results, the focus was shifted to prototype-2 and no further testing was performed on prototype-1.

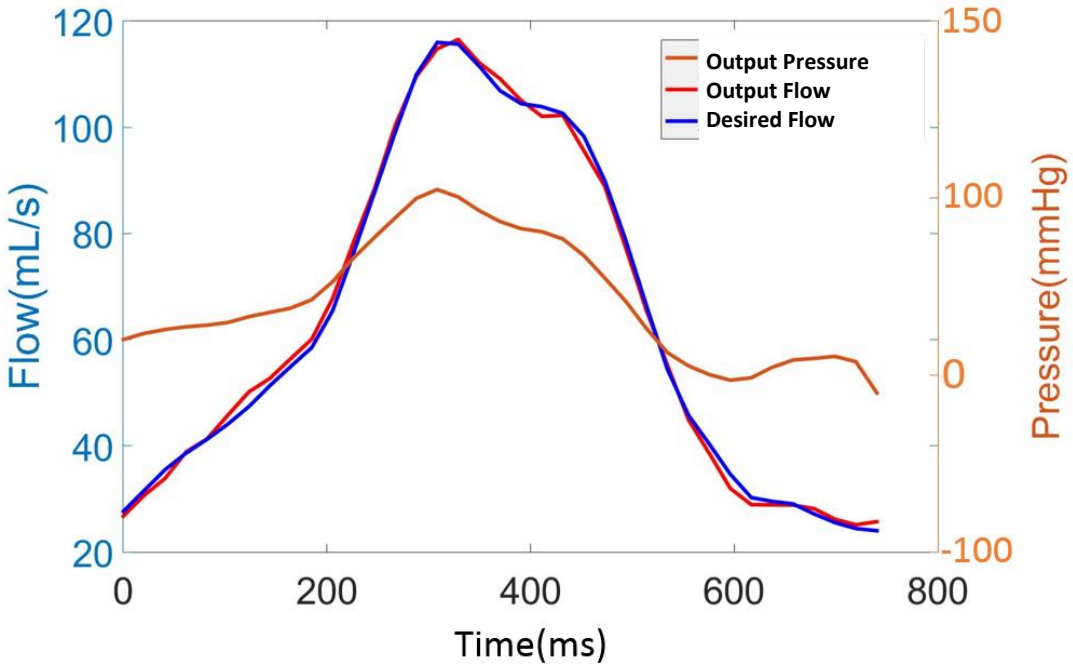

Figure 3.4: Results of Physiologically realistic test with abdominal aortic flow waveforms under exercise condition using prototype-1

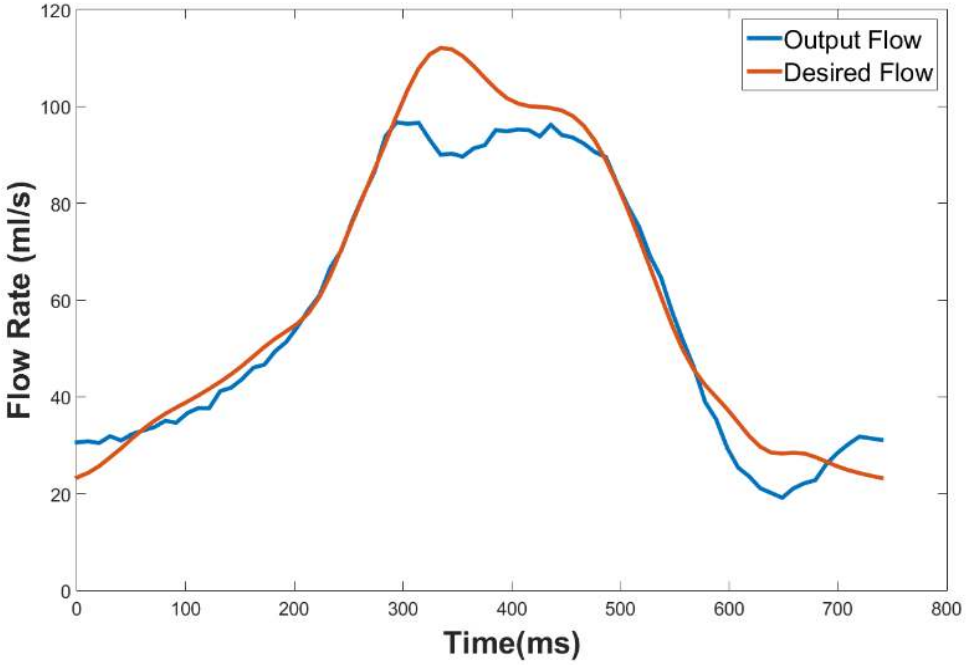

Figure 3.5: Failure in recreating flow waveform peak under higher loading conditions

CHAPTER FOUR

PROTOTYPE – 2

Design

Prototype - 2 uses a gear pump – servo motor combination (figure 4.1). Figure 4.2 shows a detailed schematic for the complete setup which is only slightly different from the previously discussed general experimental setup. The gear pump (DAYTON 4KHH8) has a rated maximum continuous output flow rate of 302ml/s. All materials used in the pump are selected to avoid reactivity with the working fluid. Detailed specifications of the pump are given in the appendix. Gear pumps can generate negative flows by changing the motor's direction of rotation and unlike piston pumps, they can be operated continuously and do not need complex tubing connections or valves for switching flow directions. Compared to the custom made piston pump in the previous prototype, the gear pump's reliability is also superior since it is designed for operation in harsh industrial conditions for long periods of time.

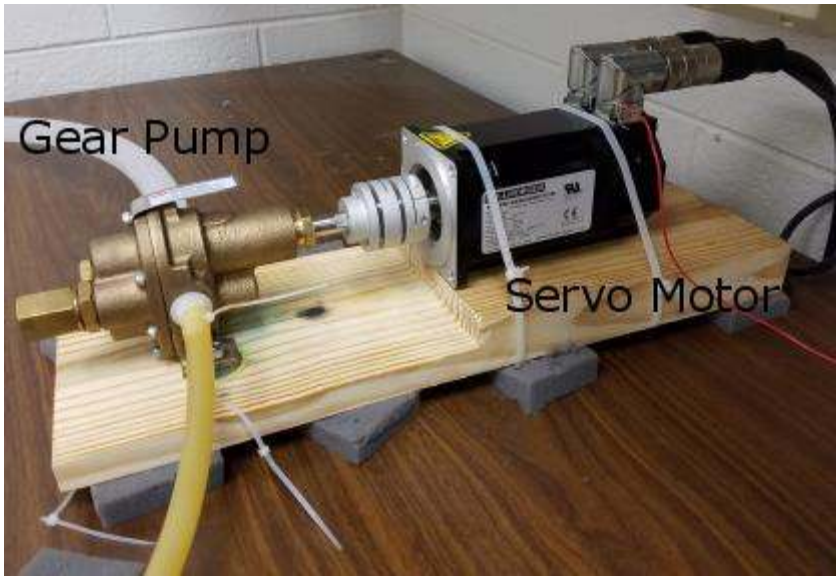

Figure 4.1: Actual image of prototype - 2

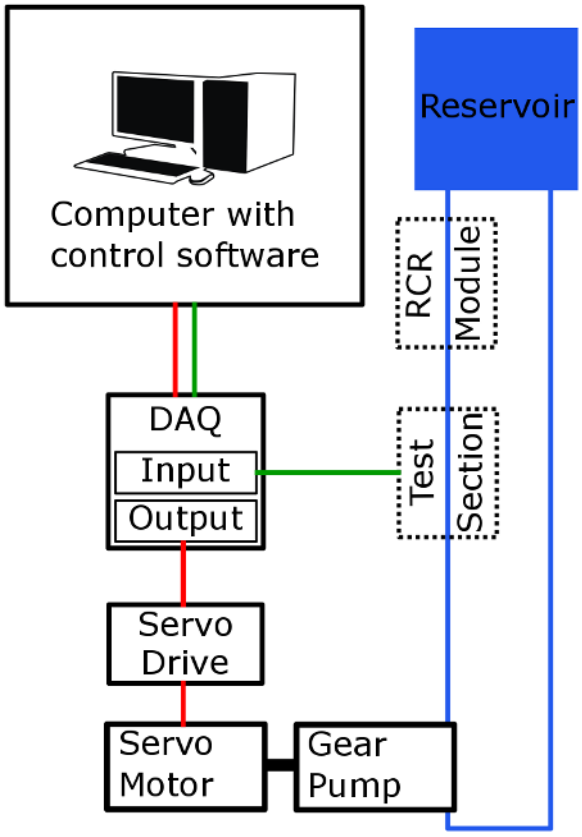

Figure 4.2: Schematic for complete experimental setup for prototype - 2

We used a triple pole servo motor (AKM42E-ANCNC-00, Kollmorgen Corporation, Radford, VA, USA) with a rated torque of 3.32Nm at 4000rpm. The servo controller accurately tracks the motor motion and is advantageous over stepper motors, which are unreliable under higher loading conditions due to the possibility of skipped steps as seen in the previous prototype. Servo motors also offer smoother motion compared to stepper motors. The chosen motor produces approximately 0.81HP at 1725 RPM. This offers significant headroom over the pump's power requirement (0.5HP for 302ml/s flow at 1300mmHg outlet pressure), and enables the pump to handle waveforms with steep acceleration. The motor is controlled using a servo drive (AKD-P00306-NBAN-0000, Kollmorgen Corporation, Radford, VA, USA) that accepts an analog voltage signal from NI 9263 as the control signal. The motor and pump shafts are coupled with a servomotor coupling (Servoclass SC 040, Zero-Max, Inc., Plymouth, MN, USA) to allow for small parallel and angular misalignment while ensuring zero backlash. The total cost, including all parts and machining is below $3000.

Results

Pump calibration was performed by running the pump at a series of constant speeds from -1400 to +1400rpm at an interval of 200rpm for a period of 5s each. This was repeated with the downstream valve partly closed to induce back pressure up to 165mmHg at 170ml/s flow rate. Figure 4.3 shows that the relationship between motor RPM and flow rate is linear within the operating range. Also, back pressure has a minimal effect on flow output, which is expected since the gear pump is designed to

operate with extremely large back pressures while maintaining the flow rate. The relationship between motor speed and pump output flow rate, shown in equation 7, was derived from this result and is used to predict the initial control waveform for all desired flow waveforms.

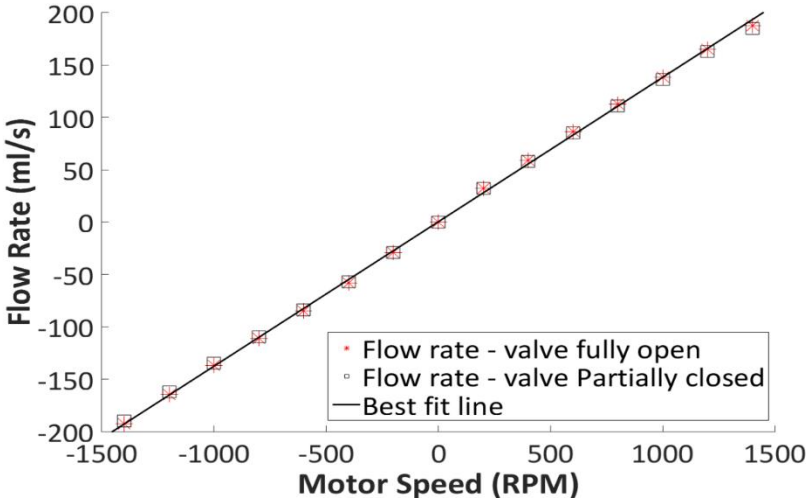

Figure 4.3: Calibration curve: Motor Speed vs Flow Rate with downstream valve fully open (blue square) and partially closed (red star)

$$Motor\ speed\ (RPM) = Flow\ Rate\ (ml/s) * 7.252 \quad (7)$$

The impulse response of the pump was analyzed to determine the maximum achievable acceleration. This value can be used to assess the pump's capability of recreating a waveform by examining the maximum acceleration present in the waveform. A step waveform from 0 to 190ml/s was used for this test. The pump required 0.1345s to achieve this change in flow rate, implying a maximum acceleration of 1412.64ml/s^2.

The semi-real time feedback algorithm was analyzed by tracking changes in the output abdominal aortic flow waveform under exercise condition in each iteration. Figure

4.4a shows the difference between the output flow waveform without any feedback and that after 6 iterations of the feedback loop, with the latter being nearly identical to the desired flow waveform. Figure 4.4b shows that the normalized RMS error generally decreases with iterations and converges around 4-7 iterations. In this example case, feedback loop increased the accuracy of the output flow waveform and reduced the error from 6.2% with no feedback to 0.71% after 6 feedback iterations. This feedback capability will be especially useful in cases where the waveform may be distorted by a longer or more compliant tubing connecting the pump and test section.

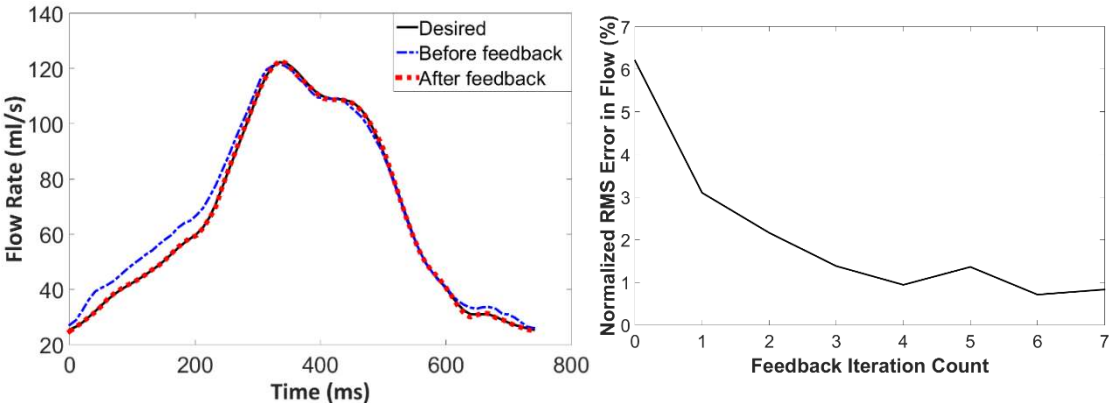

Figure 4.4a: Comparison of desired flow (solid black line) with output flow without feedback (dotted blue line) and output flow after 6 iterations of feedback (dotted red line)

Fig 4.4b: Convergence of the output flow waveform

An abdominal aortic waveform under resting condition was used to assess the ability of the pump to replicate complex waveforms with negative flow regions. The result (figure 4.5) shows that the pump successfully recreated negative flow with a normalized RMS error of 2.72% over the cycle and an R^2 value of 0.9997. This result

also shows the pump's capability to produce small amplitude oscillations typically present in human aortic waveforms.

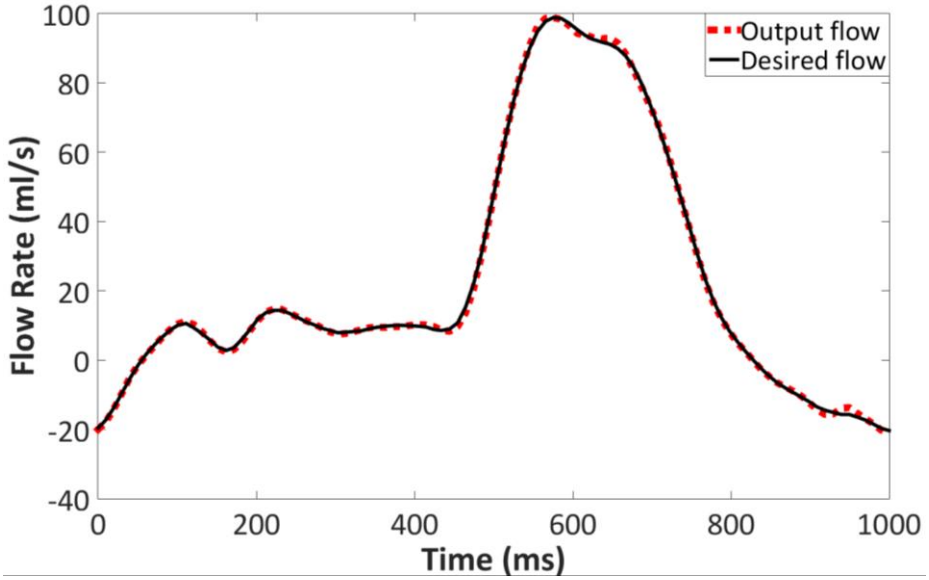

Figure 4.5: Recreation of abdominal aortic waveform under resting condition. Comparison of desired (solid black line) and output flow (dotted red line) waveforms

We demonstrate a physiologically realistic scenario featuring abdominal aortic flow and pressure waveforms under exercise condition. An RCR module was used to provide physiologically realistic downstream impedance. The compliance chamber was tuned according to the study by Kung et al. [12] and the resistances were manually tuned to obtain the required pressure ranges. Under this realistic downstream pressure condition, the pump accurately reproduced the flow waveform with a normalized RMS error of approximately 1.08% and an R^2 value of 0.9995 (figure 4.6).

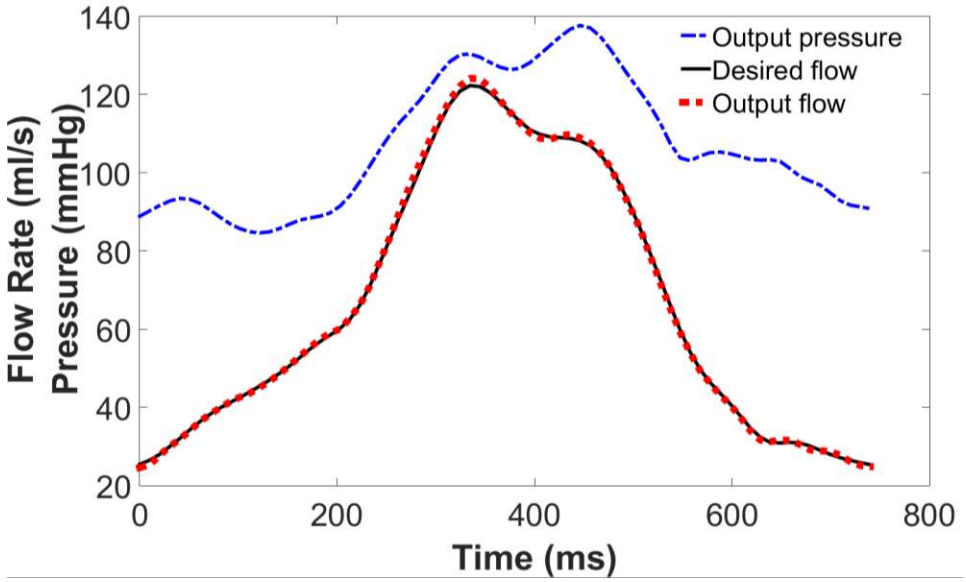

Figure 4.6: Results from physiological testing. Desired flow (solid black line) compared to output flow (dotted red line) and pressure (dotted blue line)

The cycle-to-cycle consistency of the output flow waveform is shown in figure 4.7 by superposing 20 individual waveforms from a series of consecutive waveforms. The deviation in flow rate at each time point was calculated by using the maximum and minimum values of flow across the 20 cycles. The results show a normalized RMS deviation of 3.4% and an R^2 value of 0.9895 which implies a high uniformity across waveforms produced in each cycle.

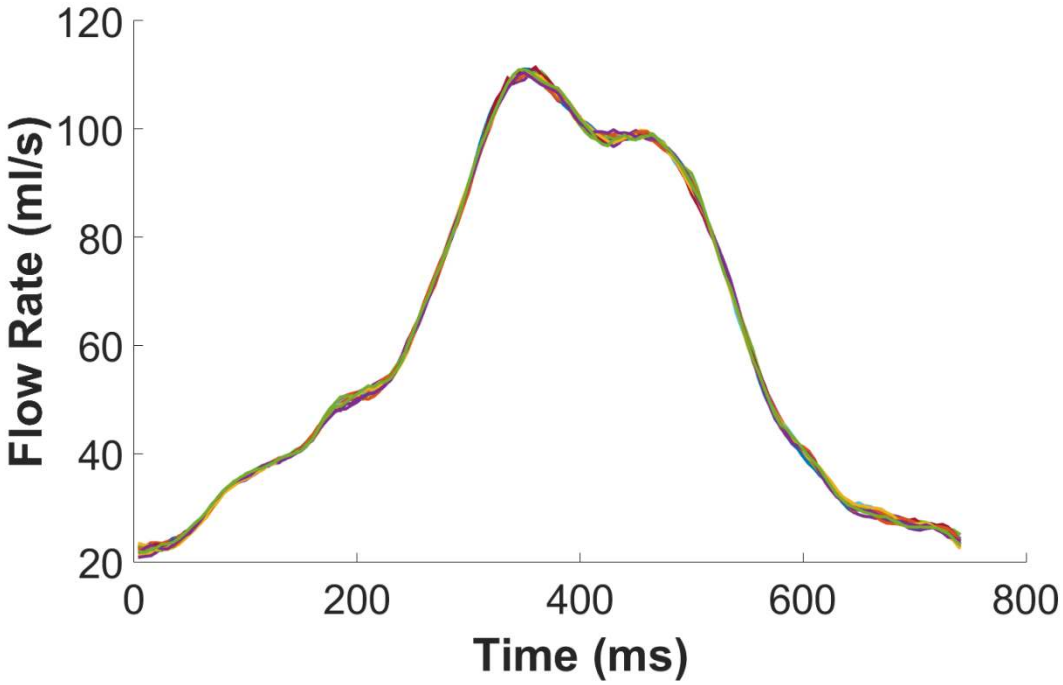

Figure 4.7: Twenty individual waveforms from a series of continuous waveforms superposed over each other to show the cycle-to-cycle consistency in output flow

The quantitative results from these tests show that the new pump performs better than or as good as the previous studies in all aspects. The peak flow rate of 302ml/s is on par with the best [8, 9]. The physiologically realistic flow accuracy at ±1% to ±2% is better than those in previous studies (±1% to ±15%) and most commercial systems (±2% to ±4%). This pump also has several nontechnical advantages over those in previous studies. It takes less than two minutes from when the desired waveform is specified for the pump to produce an accurate replica. After initial setup, no additional human intervention is necessary, and the pump can be completely controlled by computational programs. This is useful for experimental setups where large numbers of flow waveforms are to be tested in an automated framework. This pump is also considerably more affordable than commercial pumps.

Limitations

Even though the feedback algorithm increases output accuracy, it occasionally causes a distortion of the control waveform due to an accumulation of sensor noise. This is solvable by further investigation and modification of the feedback algorithm. The current pump is optimized for flow rates between 50 – 300ml/s. Flow waveforms below 50 ml/s or above 300 ml/s need to be reproduced by using smaller or larger gear pumps respectively. Therefore, the current design can be modified to service other ranges of flow rates by switching only the gear pump at a fraction (15%) of the cost of the whole setup. Even though the pump is theoretically capable of producing a peak flow rate of 300ml/s, we were only able to test the pump performance up to 170 ml/s due to the limitation of the flow sensor used.

CHAPTER FIVE

CONCLUSION

Summary

In this study, we successfully designed, built and comprehensively tested a real – time, fully programmable, pulsatile flow pump that can produce realistic physiologic flow waveforms under physiologic downstream impedances. While being more affordable than current commercial pumps, our design is capable of reproducing flow waveforms containing backflow as well as high frequency oscillations with less than 2% error. The pump can quickly create accurate reproductions of the desired waveform with minimal human interaction. The pump is controlled using commercial software and can be integrated with other computational programs, making it suitable for use in a fully automated framework. Future work will consist of testing the setup under wider flow ranges using different gear pumps and flow sensors, improving the feedback algorithm to prevent control waveform divergence due to sensor noise and reducing the pressure ripples due to vibrations.

APPENDICES

Appendix A

Flow Sensor Information

ME-PXL Series Clamp-on Flowsensors

Transonic® PXL Clamp-on Tubing Flowsensors clip on the outside of flexible laboratory tubing. No physical contact is made with the fluid media. A thin smear of Vaseline® or petroleum jelly should be applied to the section of tubing where the Sensor is applied to provide a good seal between the transducers and the tube for best ultrasonic signal transmission. PXL-Series Flowsensors can be factory calibrated and programmed for up to 4 different fluid, temperature, tubing, and flow rate combinations. Sensor size is determined by the outside diameter of the tubing. Standard PXL Sensors are sized in 1/16" increments. Metric sizes are available for metric tubing.

Easy clip on application of PXL Sensor to tubing

SENSOR SIZE	PHYSICAL SPECIFICATIONS[1]					
	DIMENSION ALONG TUBE		DEPTH		LENGTH	
	in	mm	in	mm	in	mm
2PXL	0.8	21	0.7	17	1.3	32
3PXL	0.8	21	0.7	17	1.3	32
4PXL	0.9	23	0.8	20	1.4	35
5PXL	0.9	23	0.8	20	1.4	35
6PXL	1.0	24	0.9	23	1.5	39
7PXL	1.0	26	1.0	25	1.7	42
8PXL	1.1	28	1.0	24	1.7	44
9PXL	1.3	33	1.0	25	1.8	47
10PXL	1.2	32	1.1	27	2.0	51
11PXL	1.4	35	1.1	28	2.2	56
12PXL	1.5	38	1.2	31	2.4	61
14PXL	1.6	41	1.4	36	2.6	66
16PXL	1.9	47	1.5	39	3.0	75
20PXL	2.3	58	1.8	46	3.7	93

1. Standard cable length is 2 meters.

APPLICATIONS

- Artificial Heart & VAD Performance
- Medical Device & Pump Engineering
- Manufacturing & Compliance Flow Testing

SENSOR SIZE	BIDIRECTIONAL FLOW OUTPUTS				SYSTEM ACCURACY SPECIFICATIONS[2]			ULTRASOUND FREQUENCY
	RESOLUTION[1]	LOW FLOW (¼ SCALE)	STANDARD FLOW SCALE	MAX FLOW (STD SCALE)	MAX ZERO OFFSET	ABSOLUTE ACCURACY	LINEARITY	
	ml/min	1V output in ml/min	1V output in ml/min	5V output in L/min	ml/min	% of reading	%	MHz
2PXL	0.5	50	200	1	± 4.0	± 10	± 4	3.6
3PXL	1.0	100	400	2	± 8.0	± 10	± 4	3.6
4PXL	1.0	100	400	2	± 8.0	± 10	± 4	2.4
5PXL	1.0	100	400	2	± 8.0	± 10	± 4	2.4
6PXL	2.5	250	1 L	5	± 15	± 10	± 4	2.4
7PXL	5	500	2 L	10	± 30	± 10	± 4	1.8
8PXL	5	500	2 L	10	± 30	± 10	± 4	1.8
9PXL	5	500	2 L	10	± 30	± 10	± 4	1.8
10PXL	10	1 L	4 L	20	± 60	± 10	± 4	1.2
11PXL	10	1 L	4 L	20	± 60	± 10	± 4	1.2
12PXL	10	1 L	4 L	20	± 60	± 10	± 4	1.2
14PXL	25	2.5 L	10 L	50	± 150	± 10	± 4	1.2
16PXL	25	2.5 L	10 L	50	± 150	± 10	± 4	1.2
20PXL	50	5 L	20 L	100	± 300	± 10	± 4	0.9

Calibration is dependent on tubing material, wall thickness, ultrasound velocity of liquid flowing through the tube & temperature.

1. Resolution represents the smallest detectable flow change at 0.1 Hz filter (average flow output).
2. Stated system accuracy specifications apply to PXL Flowsensors with TS410 Flow Modules. (a) Absolute accuracy is comprised of zero stability, resolution and linearity effects. Stated values apply when flow rate is greater than 5% of maximum range and zero offset is nulled. (b) If the Sensor is calibrated on-site with the system Flow Module for the tubing and liquid in use, absolute accuracy may be improved to the Linearity value. (c) On-site calibration is recommended if the Sensor is routinely used to measure flows less than 5% of the maximum range to account for non-linearities associated with flow profile.

Appendix B

Stepper Motor Specifications

87000 Series: Size 34 Linear Actuator

Haydon kerk

HaydonKerk Motion Solutions™ · www.HaydonKerk.com · Phone: 800.243.2715 · International: 203.756.7441

Size 34 Captive Shaft

Size 34 Non-Captive Shaft

Size 34 External Linear

87000 Series, Size 34... our largest, most powerful linear actuator is also available with a captive, non-captive, and external linear shaft design

Despite its large size and strength, this motor incorporates the same precision, high performance and durable patented designs featured in our entire hybrid product line.

The 87000 series delivers forces up to 500 lbs. (2224 N) in a compact, 3.4-in (87 mm) square package.

The 87000 Series is available in a wide variety of resolutions - from 0.0005-in (.0127 mm) per step to 0.005-in (.127 mm) per step. Speeds exceed 3.0-in (7.62 cm) per second.

In addition to our standard configurations, HaydonKerk Motion Solutions™ can custom build this powerful motor to meet your specific motion requirements. The in-house design and engineering team is available to assist you with a solution to fit your needs and your budget.

Salient Characteristics

Size 34: 87 mm (3.4-in) Hybrid Linear Actuator (1.8° Step Angle)						
Part No.	Captive	87H4(X)-V			87H6(X)-V	
	Non-captive	87F4(X)-V			87F6(X)-V	
	External Lin.	E87H4(X)-V			E87H6(X)-V	
Wiring		Bipolar			Unipolar*	
Winding voltage		2.85 VDC	5 VDC	12 VDC	5 VDC	12 VDC
Current/phase		5.47 A	3.12 A	1.3 A	3.12 A	1.3 A
Resistance/phase		0.52 Ω	1.6 Ω	9.23 Ω	1.6 Ω	9.23 Ω
Inductance/phase		2.86 mH	8.8 mH	51 mH	4.4 mH	25.5 mH
Power consumption		31.2 W				
Rotor inertia		1760 gcm²				
Temperature rise		135°F Rise (75°C Rise)				
Weight		5.1 lbs. (2.3 Kg)				
Insulation resistance		20 MΩ				

** Unipolar drive gives approximately 30% less thrust than bipolar drive.

Linear Travel / Step Screw Ø.625"(15.88 mm) inches	mm	Order Code I.D.
.0005	.0127	3
.000625	.0158*	B
.00125	.0317*	C
.0025	.0635	Y
.005	.127	Z

*Values truncated

Standard motors are Class B rated for maximum temperature of 130°C.

Special drive considerations may be necessary when leaving shaft fully extended or fully retracted.

Appendix C

Gear Pump Specifications

Dayton® Light-Duty Pedestal Rotary Gear Pumps

Description

Dayton rotary gear pumps features self priming and positive displacement, designed to handle high viscous fluids. They are used in wide variety of applications including industrial, agricultural, marine, domestic and commercial apartments. The pumps can be used for low speed operation with pulseless flow. Pumps are bidirectional.

Bronze: Bronze type pumps are ideal for handling water based fluids. The shafts are made of 303-SS grade with PTFE (Polytetrafluoroethylene) seal. Wet end parts are brass 303-SS, bronze gear, PTFE and carbon. These models can withstand temperature from -20 to 210°F.

Cast Iron: Cast Iron pumps are designed for handling oil based fluids not to be used with water based fluid. These models have steel spur gears with steel shafts, Viton lip seal or PTFE seal. Viton has a temperature range of 32 to 280°F and PTFE has a temperature range of -20 to 210°F. The wet end parts are constructed from CI, steel, cellulose gasket and Viton or PTFE.

Figure 1. 4KHK1 to 4KHK6

Figure 2. 4KHG4 to 4KHH6

Figure 3. 4KHJ4 to 4KHJ9

Figure 4. 4KHH7 to 4KHJ3

PERFORMANCE

GPM PUMPING 10 Wt.Oil at 70°F

BRONZE MODELS	CAST IRON MODELS	PORT SIZE *	Max Input Torque in-lbs.	RPM	Suction Lift (ft) **	FREE FLOW		25 PSI		50 PSI		75 PSI		100 PSI	
						GPM	HP	GPM	HP	GPM	HP	GPM	HP	GPM	HP
4KHG4	4KHK1	1/4"	45	900	1.5	1.2	1/6	1.0	1/6	0.8	1/6	0.6	1/4	0.4	1/3
4KHH1	4KHJ4			1200	2.0	1.6	1/6	1.5	1/6	1.4	1/4	1.3	1/4	1.2	1/3
4KHH7				1725	2.5	2.2	1/6	2.1	1/4	2.0	1/4	2.0	1/3	1.9	1/3
4KHG5	4KHK2	1/4"	45	900	1.5	2.5	1/4	2.5	1/4	2.4	1/3	2.3	1/3	2.1	1/2
4KHH2	4KHJ5			1200	2.2	3.3	1/3	3.3	1/3	3.2	1/2	3.1	1/2	2.9	3/4
4KHH8				1725	3.5	4.8	1/2	4.8	1/2	4.7	3/4	4.6	3/4	4.4	1
4KHG6	4KHK3	3/8"	90	900	2.8	3.7	1/3	3.6	1/3	3.5	1/2	3.4	1/2	3.2	3/4
4KHH3	4KHJ6			1200	5.7	4.9	1/2	4.8	1/2	4.7	3/4	4.6	3/4	4.4	1
4KHH9				1725	7.9	7.0	3/4	6.9	3/4	6.8	1	6.7	1	6.5	1-1/2
4KHG7	4KHK4	1/2"	90	900	5.1	5.6	1/3	5.5	1/3	5.4	1/2	5.3	1/2	5.0	3/4
4KHH4	4KHJ7			1200	6.7	7.5	1/2	7.4	1/2	7.3	3/4	7.2	3/4	6.9	1
4KHJ1				1725	12.3	10.8	3/4	10.7	3/4	10.6	1	10.5	1	10.2	1-1/2
4KHG8	4KHK5	3/4"	160	900	6.6	10.8	3/4	10.6	1	10.5	1	10.4	1	10.0	1
4KHH5	4KHJ8			1200	9.3	14.3	1	14.2	1	14.1	1-1/2	13.9	1-1/2	13.5	2
4KHJ2				1725	15.2	20.6	1-1/2	20.5	1-1/2	20.3	2	20.2	2	19.8	2
4KHG9	4KHK6	1"	160	900	8.1	12.6	1	12.5	1	12.3	1	12.1	1	11.7	2
4KHH6	4KHJ9			1200	11.7	16.7	1	16.6	1	16.4	1-1/2	16.2	2	15.8	2
4KHJ3				1725	19.5	24.8	1-1/2	24.7	1-1/2	24.5	2	24.3	2	23.1	3

Appendix D

Servo Motor Specifications

Specifications

	AKM41E	AKM41H	AKM42E	AKM42G	AKM43H	AKM44E
Continuous Current at Stall (A)	2.85	5.6	2.74	4.8	5.4	2.9
Peak Current at Stall (A)	11.4	22.4	11	19.2	21.6	11.4
Continuous Torque at Stall N • m (lb-in.) @ 100 °C	2.02 (17.9)	2.06 (18.2)	3.42 (30.3)	3.53 (31.2)	4.82 (42.7)	5.76 (51.0)
Peak Torque at Stall N • m (lb-in.)	6.28 (55.6)	6.36 (56.3)	11.3 (99.7)	11.5 (102)	16.1 (102)	19.9 (179)
Max Rated DC Bus Voltage	640 (480)	320 (240)	640 (480)	640 (480)	640 (480)	640 (480)
Rated Speed RPM 160 VDC (120 VAC)	1200	3000	n/a*	n/a*	1930	n/a*
Rated Speed RPM 320 VDC (240 VAC)	3000	6000	1900	3500	3860	1200
Max Continuous Power kW(HP) @160 VDC (120VAC)	0.24 (0.33)	0.58 (0.78)	n/a*	n/a*	0.56 (0.751)	n/a*
Max Continuous Power kW(HP) @320 VDC (240VAC)	0.57 (0.77)	1.02 (1.36)	0.59 (0.79)	1.06 (1.42)	1.21 (1.62)	0.66 (0.88)
Rotor Inertia (Jm) kg-cm^2 (lb*in.*s^2)	0.81 (000719)	0.81 (000719)	1.45 (0.00128)	1.45 (0.00128)	2.09 (0.00185)	2.73 (0.00242)
DC Resistance Ohms @ 25 °C (line to line)	6.02	1.56	7.78	2.51	2.1	8.64
Winding Inductance mH	18.4	5.0	26.8	9.2	8.75	33.9
Back EMF Constant V/krpm	42.9	22.4	76.2	44.7	57.4	123.0
Max Winding Temperature °C	155					
Thermal Resistance °C/W	1.04	1.04	0.89	0.89	0.7	0.71
Weight kg (lbs)	2.44 (5.4)	2.44 (5.4)	3.39 (7.5)	3.39 (7.5)	4.35 (9.59)	5.3 (11.7)
Maximum Mechanical Speed RPM	8000					
Max Radial Force (N)	500					
Max Axial Force (N)	1400					
Shaft	Smooth Shaft					
Cables	Motor-Mounted Rotatable IP65 Connectors					
Recommended Heat Sink Size	10 by 10 by ¼ in. Aluminum Plate					

*n/a indicates windings do not support voltage

REFERENCES

1. Mozaffarian D, Benjamin EJ, Go AS, et al. *Heart Disease and Stroke Statistics--2015 Update: A Report From the American Heart Association*. Vol 131.; 2014.
2. Glagov S, Zarins C, Giddens D, Ku D. Hemodynamics and atherosclerosis. Insights and perspectives gained from studies of human arteries..pdf. *Arch Pathol Lab Med*. 1988;112(10):1018-1031. http://zarinslab.stanford.edu/publications/zarins_bib/zarins_pdf/1980s/glagov_aplm_aplm_1988.pdf.
3. Groves EM, Falahatpisheh A, Su JL, Kheradvar A. The Effects of Positioning of Transcatheter Aortic Valves on Fluid Dynamics of the Aortic Root. *Asaio J*. 2014;60(5):545-552 10.1097
4. Pahlevan NM, Gharib M. In-vitro investigation of a potential wave pumping effect in human aorta. *J Biomech*. 2013;46(13):2122-2129. doi:10.1016/j.jbiomech.2013.07.006.
5. Kung E, Pennati G, Migliavacca F, et al. A Simulation Protocol for Exercise Physiology in Fontan Patients Using a Closed Loop Lumped-Parameter Model. *J Biomech Eng*. 2014;136(8):81007. http://dx.doi.org/10.1115/1.4027271.
6. Kefayati S, Poepping TL. 3-D flow characterization and shear stress in a stenosed carotid artery bifurcation model using stereoscopic PIV technique. *2010 Annu Int Conf IEEE Eng Med Biol Soc EMBC'10*. 2010:3386-3389. doi:10.1109/IEMBS.2010.5627933.
7. Frayne R, Holdsworth DW, Gowman LM, et al. Computer-controlled flow

simulator for MR flow studies. *J Magn Reson Imaging*. 1992;2(5):605-612. doi:10.1002/jmri.1880020522.

8. Hoskins PR, Anderson T, McDicken WN. A computer controlled flow phantom for generation of physiological Doppler waveforms. *Phys Med Biol*. 1989;34(11):1709-1717. doi:10.1088/0031-9155/34/11/018.

9. Eriksson A, Persson HW, Lindstrom K. A computer-controlled arbitrary flow wave form generator for physiological studies. *Rev Sci Instrum*. 2000;71(1):235-242. doi:10.1063/1.1150189.

10. Tsai W, Savaş O. Flow pumping system for physiological waveforms. *Med Biol Eng Comput*. 2010;48(2):197-201. doi:10.1007/s11517-009-0573-6.

11. Kung EO, Taylor CA. Development of a Physical Windkessel Module to Re-Create In Vivo Vascular Flow Impedance for In Vitro Experiments. *Cardiovasc Eng Technol*. 2011;2(1):2-14. doi:10.1007/s13239-010-0030-6.

12. Kung EO, Les AS, Medina F, Wicker RB, McConnell M V, Taylor C a. In vitro validation of finite-element model of AAA hemodynamics incorporating realistic outlet boundary conditions. *J Biomech Eng*. 2011;133(4):041003. doi:10.1115/1.4003526.